Comparison of Single-point and Two-point Difference Track Initiation Algorithms Using Position Measurements

MALLICK Mahendra[1] LA SCALA Barbara[2]

Abstract We consider the problem of initializing the tracking filter of a target moving with nearly constant velocity when position-only ($1D$, $2D$, or $3D$) measurements are available. It is known that the Kalman filter is optimal for such a problem, provided it is correctly initialized. We compare a single-point and the well-known two-point difference track initialization algorithms. We analytically show that if the process noise approaches zero and the maximum speed of a target used to initialize the velocity variance approaches infinity, then the single-point algorithm reduces to the two-point difference algorithm. We present numerical results that show that the single-point algorithm performs consistently better than the two-point difference algorithm in the mean square error sense. We also present analytical results that support the conjecture that this is true in general.

Key words Track initiation, Kalman filter, unbiased estimator, minimum mean square error

Track initiation is an essential component of all tracking algorithms, but one that has received little attention. For situations where the dynamic and measurement models are linear and appropriate Gaussianity and independence assumptions hold, it is well-known that the Kalman filter (KF) is optimal in the minimum mean squared error sense[1−2]. However, this result requires that the mean of the initial state estimate is equal to the mean of the initial state, and its associated error covariance matrix is equal to the true initial covariance. In practice, this is rarely the case. Ideally, any initial transients introduced by incorrect initialization will quickly be eliminated, but this cannot be guaranteed. The effect of such errors on Kalman filters for general problems have been examined in [3 − 5] and more recently, with a focus on target tracking, in [6].

There are additional factors to be considered for target tracking problems. In real-world radar tracking problems, the measurements are range and azimuth in the $2D$ case, and range, azimuth, and elevation in the $3D$ case. Unbiased position measurements and associated measurement covariances can be derived from these radar measurements[7], but the associated measurement errors are no longer Gaussian. For the ground target tracking problem using the ground moving target indicator (GMTI) radar sensor, the $3D$ position of a target can be estimated using the GMTI range and azimuth measurements, sensor position, and terrain data[8]. A similar situation occurs in the video tracking problem. The $3D$ position of a ground target can be estimated using the target centroid pixel location, intrinsic and extrinsic camera parameters, and terrain data[9]. Similarly, the errors in the $3D$ position estimate of the target for the GMTI and video tracking problems are not Gaussian. This lack of Gaussianity will also have an impact on the performance of the filter and can potentially exacerbate any initialization errors. This is demonstrated in [10], which considers the problem of target tracking with long range radars.

In this paper, we compare two track initiation algorithms, the single-point (SP) method[11−12] and the two-point difference (TPD) method[2], using position-only measurements in $1D$, $2D$, or $3D$. We assume that the target motion is described by the nearly constant velocity model (NCVM)[2]. Then, the SP algorithm initiates the track using the first position measurement and sets the velocity components to zero. The maximum possible speed of the target is used, in addition to the measurement covariances, to initialize the associated covariance matrix[11−12]. A KF is then used to process subsequent position measurements. In contrast, the TPD algorithm[2] uses information on the first two measurements alone to initialize the filter. This estimate represents the maximum likelihood estimate for Gaussian position errors. We demonstrate numerically that the SP method has a smaller mean square error matrix (MSEM) than the TPD for a $3D$ radar target tracking problem. We conjecture that this result holds analytically. We analytically show that, if the process noise approaches zero and the maximum speed of a target used to initialize the velocity variance approaches infinity, then the SP algorithm reduces to the TPD algorithm.

The organization of the paper is as follows. Section 1 describes the target dynamic and measurement models. Section 2 presents the SP and TPD track initiation algorithms. The bias and the MSEM of the two estimators at the second observation time are discussed in Section 3. Section 4 establishes the relationship between the two track initiation algorithms analytically. Finally, Sections 5 and 6 present numerical results and conclusions.

Let n (1, 2 or 3) denote the dimension of the target position. We use I and 0_n to represent the $n \times n$ identity matrix and null matrix, respectively. A general $m \times n$ null matrix is denoted by $0_{m\times n}$.

1 Dynamic and measurement models

We consider the NCVM in n dimensions and use the discretized continuous-time dynamic model[2]. Then, the position $\boldsymbol{p}_k \in \mathbf{R}^n$ and velocity $\boldsymbol{v}_k \in \mathbf{R}^n$ of a target define target state $\boldsymbol{x}_k \in \mathbf{R}^{2n}$ at time t_k

$$\boldsymbol{x}_k = \left[\begin{array}{cc} \boldsymbol{p}_k^{\mathrm{T}} & \boldsymbol{v}_k^{\mathrm{T}} \end{array} \right]^{\mathrm{T}} \tag{1}$$

Received September 13, 2007; in revised form January 14, 2008
1. 1048 Highland Drive, Del Mar CA 92014, USA 2. Melbourne Systems Laboratory, Department of Electrical and Electronic Engineering, University of Melbourne, Victoria, 3010, Australia
DOI: 10.3724/SP.J.1004.2008.00258

The continuous-time NCVM is formally described by [2, 13 − 14]

$$\frac{\mathrm{d}\boldsymbol{x}(t)}{\mathrm{d}t} = A\boldsymbol{x}(t) + G\tilde{\boldsymbol{w}}(t) \tag{2}$$

where

$$A = \begin{bmatrix} 0_n & I \\ 0_n & 0_n \end{bmatrix} \tag{3}$$

$$G = \begin{bmatrix} 0_n \\ I \end{bmatrix} \tag{4}$$

$$\tilde{\boldsymbol{w}}(t) = \begin{bmatrix} \tilde{w}_1(t) \\ \vdots \\ \tilde{w}_n(t) \end{bmatrix} \tag{5}$$

For the NCVM, $\tilde{w}_i(t)$ in (5) represents a zero-mean white noise acceleration along the i-th axis with power spectral density $q_i, i = 1, \cdots, n$[2]. Axis 1, 2, and 3 correspond to the X, Y, and Z axes, respectively. We assume that $\tilde{w}_i(t)$ and $\tilde{w}_j(t)$ for $i \neq j$ are uncorrelated. Thus, we have

$$\mathrm{E}[\tilde{w}_i(t)] = 0, \quad i = 1, \cdots, n \tag{6}$$

$$\mathrm{E}[\tilde{w}_i(t)\tilde{w}_j^{\mathrm{T}}(t)] = \delta_{ij}\delta(t-\tau)q_i, \quad i, j = 1, \cdots, n \tag{7}$$

where the δ with the suffixes is a Kronecker delta and the δ with the argument is a Dirac delta. Discretization of the continuous-time NCVM in (2) at measurement times $\{t_k\}$ yields[2, 14]

$$\boldsymbol{x}_k = F_{k,k-1}\boldsymbol{x}_{k-1} + \boldsymbol{w}_{k,k-1}, \quad k = 2, 3, \cdots \tag{8}$$

where $F_{k,k-1}$ and $\boldsymbol{w}_{k,k-1}$ are the state transition matrix and integrated process noise for the time interval $[t_{k-1}, t_k]$, respectively[2, 14]

$$F_{k,k-1} = F(t_k, t_{k-1}) = \exp(A\Delta_k) = \begin{bmatrix} I & I\Delta_k \\ 0_n & I \end{bmatrix} \tag{9}$$

$$\boldsymbol{w}_{k,k-1} = \int_{t_{k-1}}^{t_k} F(t_k, t)G\tilde{\boldsymbol{w}}(t)\mathrm{d}t \tag{10}$$

$$\Delta_k = t_k - t_{k-1} \tag{11}$$

Since $\{\tilde{w}_j(t)\}$ are zero-mean, white, and uncorrelated, $\boldsymbol{w}_{k,k-1}$ is zero-mean, white, and Gaussian with covariance $Q_{k,k-1}$ (process noise covariance matrix)

$$\boldsymbol{w}_{k,k-1} \sim \mathcal{N}(0_{2n\times 1}, Q_{k,k-1}) \tag{12}$$

Using (7) and (10), we can show that

$$\mathrm{E}[\boldsymbol{w}_{k,k-1}\boldsymbol{w}_{l,l-1}^{\mathrm{T}}] = \delta_{kl}Q_{k,k-1} \tag{13}$$

For $n = 3$,

$$Q_{k,k-1} = \tag{14}$$

$$\begin{bmatrix} \frac{1}{3}q_1\Delta_k^3 & 0 & 0 & \frac{1}{2}q_1\Delta_k^2 & 0 & 0 \\ 0 & \frac{1}{3}q_2\Delta_k^3 & 0 & 0 & \frac{1}{2}q_2\Delta_k^2 & 0 \\ 0 & 0 & \frac{1}{3}q_3\Delta_k^3 & 0 & 0 & \frac{1}{2}q_3\Delta_k^2 \\ \frac{1}{2}q_1\Delta_k^2 & 0 & 0 & q_1\Delta_k & 0 & 0 \\ 0 & \frac{1}{2}q_2\Delta_k^2 & 0 & 0 & q_2\Delta_k & 0 \\ 0 & 0 & \frac{1}{2}q_3\Delta_k^2 & 0 & 0 & q_3\Delta_k \end{bmatrix}$$

We assume that q_i is the same for each coordinate axis, i.e.,

$$q_i = q, \quad i = 1, \cdots, n \tag{15}$$

Then

$$Q_{k,k-1} = q\begin{bmatrix} \frac{1}{3}I\Delta_k^3 & \frac{1}{2}I\Delta_k^2 \\ \frac{1}{2}I\Delta_k^2 & I\Delta_k \end{bmatrix} \tag{16}$$

The position measurement model is[2]

$$\boldsymbol{z}_k = H\boldsymbol{x}_k + \boldsymbol{n}_k = \boldsymbol{p}_k + \boldsymbol{n}_k, \quad i = 1, 2, \cdots, N \tag{17}$$

$$H = \begin{bmatrix} I & 0_n \end{bmatrix} \tag{18}$$

where $\boldsymbol{n}_k$ is a zero-mean white Gaussian measurement noise with covariance R_k with

$$\mathrm{E}[\boldsymbol{n}_k] = 0, \quad \mathrm{E}[\boldsymbol{n}_k\boldsymbol{n}_l^{\mathrm{T}}] = \delta_{kl}R_k, \ k, l = 1, 2, \cdots, N \tag{19}$$

Note that, if radar (range, azimuth) or (range, azimuth, elevation) measurements with additive Gaussian measurement noises are used, then the measurement noise associated with the converted Cartesian measurements is zero-mean but not Gaussian[7].

The state at time t_2, according to (8), is described by

$$\boldsymbol{x}_2 = F\boldsymbol{x}_1 + \boldsymbol{w} \tag{20}$$

where $F = F_{2,1}$ is the state transition matrix and $\boldsymbol{w} = \boldsymbol{w}_{2,1}$ is the zero-mean white Gaussian integrated process noise[2, 14] with covariance $Q = Q_{2,1}$ for the time interval $[t_1, t_2]$

$$F = \begin{bmatrix} I & TI \\ 0 & I \end{bmatrix} \tag{21}$$

$$T = t_2 - t_1 \tag{22}$$

$$\boldsymbol{w} \sim \mathcal{N}(0, Q) \tag{23}$$

Using (16) and (22), we get

$$Q = \begin{bmatrix} a_3 I & a_2 I \\ a_2 I & a_1 I \end{bmatrix} \tag{24}$$

where

$$a_m = \frac{qT^m}{m}, \quad m = 1, 2, 3 \tag{25}$$

Substitution of (1) and (21) in (20) gives

$$\boldsymbol{x}_2 = \begin{bmatrix} \boldsymbol{p}_2 \\ \boldsymbol{v}_2 \end{bmatrix} = \begin{bmatrix} \boldsymbol{p}_1 + T\boldsymbol{v}_1 \\ \boldsymbol{v}_1 \end{bmatrix} + \begin{bmatrix} \boldsymbol{w}_p \\ \boldsymbol{w}_v \end{bmatrix} \tag{26}$$

where

$$\boldsymbol{w} = \begin{bmatrix} \boldsymbol{w}_p \\ \boldsymbol{w}_v \end{bmatrix} \tag{27}$$

$$\boldsymbol{w}_p \sim \mathcal{N}(\boldsymbol{0}, a_3 I) \tag{28}$$

$$\boldsymbol{w}_v \sim \mathcal{N}(\boldsymbol{0}, a_1 I) \tag{29}$$

$$\mathrm{E}[\boldsymbol{w}_p\boldsymbol{w}_v^{\mathrm{T}}] = a_2 I \tag{30}$$

From (26), we get

$$\boldsymbol{p}_2 = \boldsymbol{p}_1 + T\boldsymbol{v}_1 + \boldsymbol{w}_p \tag{31}$$

$$\boldsymbol{v}_2 = \boldsymbol{v}_1 + \boldsymbol{w}_v \tag{32}$$

2 Track initialization algorithms

We assume that the initial state $\boldsymbol{x}_1$ at time t_1 is a Gaussian random variable with mean $\bar{\boldsymbol{x}}_1$ and covariance P_1,

$$\boldsymbol{x}_1 \sim \mathcal{N}(\bar{\boldsymbol{x}}_1, P_1) \tag{33}$$

Thus, in a given Monte Carlo simulation, $\boldsymbol{x}_1$ assumes a value

$$\boldsymbol{x}_1 = \bar{\boldsymbol{x}}_1 + \boldsymbol{e}_1 \tag{34}$$

where $\boldsymbol{e}_1$ is a zero-mean Gaussian random variable with covariance P_1, i.e.

$$\boldsymbol{e}_1 \sim \mathcal{N}(0, P_1) \tag{35}$$

Writing the state in terms of position and velocity, we have

$$\left[\begin{array}{c} \boldsymbol{p}_1 \\ \boldsymbol{v}_1 \end{array}\right] = \left[\begin{array}{c} \bar{\boldsymbol{p}}_1 \\ \bar{\boldsymbol{v}}_1 \end{array}\right] + \left[\begin{array}{c} \boldsymbol{e}_{1p} \\ \boldsymbol{e}_{1v} \end{array}\right] \tag{36}$$

We assume that the errors in the position and velocity are uncorrelated,

$$\boldsymbol{e}_{1p} \sim \mathcal{N}(0, P_{1p}), \quad \boldsymbol{e}_{1v} \sim \mathcal{N}(0, P_{1v}) \tag{37}$$

$$P_1 = \left[\begin{array}{cc} P_{1p} & 0 \\ 0 & P_{1v} \end{array}\right] \tag{38}$$

Let $\hat{\boldsymbol{x}}_{2|2}$ and $P_{2|2}$ denote the state estimate and covariance at t_2 after processing the measurements $\{\boldsymbol{z}_1, \boldsymbol{z}_2\}$. Next, we present the TPD and SP track initialization algorithms in Sections 2.1 and 2.2, respectively.

2.1 TPD track initialization algorithm

The TPD track initialization algorithm[2] approximates the initial track state using the first two position measurements as follows

$$\hat{\boldsymbol{x}}_{2|2}^{TPD} = \left[\begin{array}{c} \boldsymbol{z}_2 \\ \dfrac{1}{T}(\boldsymbol{z}_2 - \boldsymbol{z}_1) \end{array}\right] \tag{39}$$

The initial state error covariance is computed assuming there is no process noise, which yields

$$P_{2|2}^{TPD} = \left[\begin{array}{cc} R_2 & \dfrac{1}{T}R_2 \\ \dfrac{1}{T}R_2 & \dfrac{1}{T^2}(R_1 + R_2) \end{array}\right] \tag{40}$$

2.2 SP track initialization algorithm

In the SP algorithm[11−12], the track is initialized at t_1 by

$$\hat{\boldsymbol{x}}_{1|1} = \left[\begin{array}{c} \boldsymbol{z}_1 \\ 0_{n\times 1} \end{array}\right] \tag{41}$$

where the position component of the state is set equal to the position measurement, and the velocity component is set to zero. The covariance corresponding to $\hat{\boldsymbol{x}}_{1|1}$ is given by[11−12]

$$P_{1|1} = \left[\begin{array}{cc} R_1 & 0_n \\ 0_n & dI \end{array}\right] \tag{42}$$

$$d = \frac{v_{\max}^2}{3} \tag{43}$$

where $v_{\max}$ is the maximum possible speed of a target. Thus, $v_{\max}$ represents the *a priori* information. Next, the KF algorithm is used for prediction and update at t_2. It can be shown that the updated state estimate and its error covariance are given by

$$\hat{\boldsymbol{x}}_{2|2}^{SP} = \left[\begin{array}{c} \boldsymbol{z}_1 + K_1(\boldsymbol{z}_2 - \boldsymbol{z}_1) \\ K_2(\boldsymbol{z}_2 - \boldsymbol{z}_1) \end{array}\right] \tag{44}$$

$$P_{2|2}^{SP} = \left[\begin{array}{cc} A_1 - A_1S^{-1}A_1 & A_2 - A_1S^{-1}A_2 \\ A_2 - A_2S^{-1}A_1 & A_3 - A_2S^{-1}A_2 \end{array}\right] \tag{45}$$

where K is the Kalman gain given by

$$K = \left[\begin{array}{c} K_1 \\ K_2 \end{array}\right] = \left[\begin{array}{c} A_1S^{-1} \\ A_2S^{-1} \end{array}\right] \tag{46}$$

and S is the innovation covariance

$$S = A_1 + R_2 \tag{47}$$

and

$$A_1 = R_1 + (T^2d + a_3)I \tag{48}$$

$$A_2 = (Td + a_2)I \tag{49}$$

$$A_3 = (d + a_1)I \tag{50}$$

3 Bias and mean square error

The covariances calculated by the TPD and SP track initiation algorithm are given by (40) and (45), respectively. We assume that (8) (or (20) at t_2) and (33) $\sim$ (38) describe the correct dynamic model and prior distribution for the system. Then, we calculate the bias error and MSEM for the two track initialization algorithms relative to the truth model. The MSEM represents the actual error for each track initiation algorithm. We show that the covariances in (40) and (45) are different from the corresponding MSEMs.

The error in $\hat{\boldsymbol{x}}_{2|2}$ is defined by

$$\tilde{\boldsymbol{x}}_{2|2} = \boldsymbol{x}_2 - \hat{\boldsymbol{x}}_{2|2} \tag{51}$$

3.1 TPD track initialization algorithm

Use of (39) in (51) gives

$$\tilde{\boldsymbol{x}}_{2|2}^{TPD} = \boldsymbol{x}_2 - \left[\begin{array}{c} \boldsymbol{z}_2 \\ \dfrac{1}{T}(\boldsymbol{z}_2 - \boldsymbol{z}_1) \end{array}\right] = \tag{52}$$

$$\boldsymbol{x}_2 - \left[\begin{array}{c} H\boldsymbol{x}_2 + \boldsymbol{n}_2 \\ \dfrac{1}{T}(H\boldsymbol{x}_2 + \boldsymbol{n}_2 - H\boldsymbol{x}_1 - \boldsymbol{n}_1) \end{array}\right] =$$

$$\left[\begin{array}{c} \boldsymbol{p}_2 \\ \boldsymbol{v}_2 \end{array}\right] - \left[\begin{array}{c} \boldsymbol{p}_2 + \boldsymbol{n}_2 \\ \dfrac{1}{T}(\boldsymbol{p}_2 + \boldsymbol{n}_2 - \boldsymbol{p}_1 - \boldsymbol{n}_1) \end{array}\right] =$$

$$\left[\begin{array}{c} -\boldsymbol{n}_2 \\ \boldsymbol{v}_2 - \dfrac{1}{T}(\boldsymbol{p}_2 - \boldsymbol{p}_1) - \dfrac{1}{T}(\boldsymbol{n}_2 - \boldsymbol{n}_1) \end{array}\right]$$

From (31), we get

$$\frac{1}{T}(\boldsymbol{p}_2 - \boldsymbol{p}_1) = \boldsymbol{v}_1 + \frac{1}{T}\boldsymbol{w}_p \tag{53}$$

which with (32) gives

$$\tilde{\boldsymbol{x}}_{2|2}^{TPD} = \left[\begin{array}{c} -\boldsymbol{n}_2 \\ \boldsymbol{v}_2 - \boldsymbol{v}_1 - \dfrac{1}{T}\boldsymbol{w}_p - \dfrac{1}{T}(\boldsymbol{n}_2 - \boldsymbol{n}_1) \end{array}\right] = \tag{54}$$

$$\left[\begin{array}{c} -\boldsymbol{n}_2 \\ \boldsymbol{w}_v - \dfrac{1}{T}\boldsymbol{w}_p - \dfrac{1}{T}(\boldsymbol{n}_2 - \boldsymbol{n}_1) \end{array}\right]$$

Using the zero-mean properties of the measurement noise and process noise, we get

$$\mathrm{E}[\tilde{\boldsymbol{x}}_{2|2}^{TPD}] = 0_{2n\times 1} \tag{55}$$

Thus, the TPD estimator is unbiased.

Let Σ_2^{TPD} denote the MSEM of the TPD track initiation error. Then

$$\begin{aligned}\Sigma_2^{TPD} = \mathrm{E}[\tilde{\boldsymbol{x}}_{2|2}^{TPD}(\tilde{\boldsymbol{x}}_{2|2}^{TPD})^{\mathrm{T}}] = \\ \left[\begin{array}{cc} R_2 & \frac{1}{T}R_2 \\ \frac{1}{T}R_2 & \frac{1}{T^2}(R_1+R_2)+\frac{a_3}{T^2}I+a_1 I-\frac{2a_2}{T}I \end{array}\right] = \\ \left[\begin{array}{cc} R_2 & \frac{1}{T}R_2 \\ \frac{1}{T}R_2 & \frac{1}{T^2}(R_1+R_2)+\frac{qT}{3}I+qTI-qTI \end{array}\right] = \\ \left[\begin{array}{cc} R_2 & \frac{1}{T}R_2 \\ \frac{1}{T}R_2 & \frac{1}{T^2}(R_1+R_2)+\frac{1}{3}qTI \end{array}\right]\end{aligned} \tag{56}$$

Comparison of (40) and (56) shows that, the position covariance and position-velocity covariance agree. However, the velocity component of the MSEM has an additional term $\frac{1}{3}qTI$ compared with the TPD calculated covariance, which arises due to neglecting the process noise.

In [6], it is argued that a more accurate two-point based initialization method is to use $\hat{\boldsymbol{x}}_{2|2}^{TPD}$ and Σ_2^{TPD} as the initial state estimate and its associated error covariance, respectively. This initialization scheme is the solution to

$$\arg\min_{\boldsymbol{x}_2}\left(\left[\begin{array}{c}\boldsymbol{z}_2\\ \boldsymbol{z}_1\end{array}\right]-\left[\begin{array}{c}H\boldsymbol{x}_2\\ H\boldsymbol{x}_1\end{array}\right]\right)^{\mathrm{T}} W \left(\left[\begin{array}{c}\boldsymbol{z}_2\\ \boldsymbol{z}_1\end{array}\right]-\left[\begin{array}{c}H\boldsymbol{x}_2\\ H\boldsymbol{x}_1\end{array}\right]\right) \tag{57}$$

where W is a symmetric, positive definite weighting matrix chosen so that the solution to (57) minimizes

$$\mathrm{E}[(\boldsymbol{x}_2-\hat{\boldsymbol{x}}_2)(\boldsymbol{x}_2-\hat{\boldsymbol{x}}_2)^{\mathrm{T}}|\boldsymbol{x}_2] \tag{58}$$

In this formulation, $\boldsymbol{x}_2$ is treated as a random variable. In [6] this method is termed optimal Bayesian weighted least squares initialization.

3.2 SP based track initialization algorithm

Substitution of (44) into (51) gives the error in the SP initiated track state at time t_2

$$\begin{aligned}\tilde{\boldsymbol{x}}_{2|2}^{SP} = \boldsymbol{x}_2 - \hat{\boldsymbol{x}}_{2|2}^{SP} = \\ \left[\begin{array}{c}\boldsymbol{p}_2\\ \boldsymbol{v}_2\end{array}\right]-\left[\begin{array}{c}\boldsymbol{z}_1+K_1(\boldsymbol{z}_2-\boldsymbol{z}_1)\\ K_2(\boldsymbol{z}_2-\boldsymbol{z}_1)\end{array}\right] = \\ \left[\begin{array}{c}\tilde{\boldsymbol{p}}_{2|2}\\ \tilde{\boldsymbol{v}}_{2|2}\end{array}\right]\end{aligned} \tag{59}$$

Use of (17) in (59) gives

$$\tilde{\boldsymbol{x}}_{2|2}^{SP} = \left[\begin{array}{c}\boldsymbol{p}_2-(I-K_1)(\boldsymbol{p}_1+\boldsymbol{n}_1)-K_1(\boldsymbol{p}_2+\boldsymbol{n}_2)\\ \boldsymbol{v}_2-K_2(\boldsymbol{p}_2+\boldsymbol{n}_2)+K_2(\boldsymbol{p}_1+\boldsymbol{n}_1)\end{array}\right] \tag{60}$$

Thus,

$$\begin{aligned}\tilde{\boldsymbol{p}}_{2|2} = (I-K_1)\boldsymbol{p}_2-(I-K_1)\boldsymbol{p}_1-(I-K_1)\boldsymbol{n}_1-K_1\boldsymbol{n}_2 = \\ (I-K_1)(\boldsymbol{p}_2-\boldsymbol{p}_1)-(I-K_1)\boldsymbol{n}_1-K_1\boldsymbol{n}_2\end{aligned} \tag{61}$$

From (31), we have

$$\boldsymbol{p}_2-\boldsymbol{p}_1 = T\boldsymbol{v}_1+\boldsymbol{w}_p \tag{62}$$

Substitution of (62) into (61) gives

$$\begin{aligned}\tilde{\boldsymbol{p}}_{2|2} = T(I-K_1)\boldsymbol{v}_1+(I-K_1)(\boldsymbol{w}_p-\boldsymbol{n}_1)-K_1\boldsymbol{n}_2 = \\ T(I-K_1)(\bar{\boldsymbol{v}}_1+\boldsymbol{e}_{1v})+(I-K_1)(\boldsymbol{w}_p-\boldsymbol{n}_1)-K_1\boldsymbol{n}_2\end{aligned} \tag{63}$$

Taking the velocity component of $\tilde{\boldsymbol{x}}_{2|2}^{SP}$ from (59) and using (26) and (62), we get

$$\begin{aligned}\tilde{\boldsymbol{v}}_{2|2} = \boldsymbol{v}_1+\boldsymbol{w}_v-K_2(\boldsymbol{p}_2-\boldsymbol{p}_1)+K_2(\boldsymbol{n}_1-\boldsymbol{n}_2) = \\ \boldsymbol{v}_1+\boldsymbol{w}_v-K_2(T\boldsymbol{v}_1+\boldsymbol{w}_p)+K_2(\boldsymbol{n}_1-\boldsymbol{n}_2) = \\ (I-TK_2)\boldsymbol{v}_1+\boldsymbol{w}_v+K_2(\boldsymbol{n}_1-\boldsymbol{n}_2-\boldsymbol{w}_p) = \\ (I-TK_2)(\bar{\boldsymbol{v}}_1+\boldsymbol{e}_{1v})+\boldsymbol{w}_v+K_2(\boldsymbol{n}_1-\boldsymbol{n}_2-\boldsymbol{w}_p)\end{aligned} \tag{64}$$

Therefore,

$$\mathrm{E}[\tilde{\boldsymbol{x}}_{2|2}^{SP}] = \left[\begin{array}{c}\mathrm{E}[\tilde{\boldsymbol{p}}_{2|2}]\\ \mathrm{E}[\tilde{\boldsymbol{v}}_{2|2}]\end{array}\right] = \left[\begin{array}{c}T(I-K_1)\bar{\boldsymbol{v}}_1\\ (I-TK_2)\bar{\boldsymbol{v}}_1\end{array}\right] \tag{65}$$

Thus, the SP initialization state estimate $\hat{\boldsymbol{x}}_{2|2}^{SP}$ at t_2 is biased in both the position and velocity components.

Using (63) and (64), the MSEM for the SP track initiation error is

$$\Sigma_2^{SP} = \left[\begin{array}{cc}\mathrm{E}[\tilde{\boldsymbol{p}}_{2|2}\tilde{\boldsymbol{p}}_{2|2}^{\mathrm{T}}] & \mathrm{E}[\tilde{\boldsymbol{p}}_{2|2}\tilde{\boldsymbol{v}}_{2|2}^{\mathrm{T}}]\\ \mathrm{E}[\tilde{\boldsymbol{p}}_{2|2}^{\mathrm{T}}\tilde{\boldsymbol{v}}_{2|2}] & \mathrm{E}[\tilde{\boldsymbol{v}}_{2|2}\tilde{\boldsymbol{v}}_{2|2}^{\mathrm{T}}]\end{array}\right] \tag{66}$$

where

$$\mathrm{E}[\tilde{\boldsymbol{p}}_{2|2}\tilde{\boldsymbol{p}}_{2|2}^{\mathrm{T}}] = T^2(I-K_1)(\bar{\boldsymbol{v}}_1\bar{\boldsymbol{v}}_1^{\mathrm{T}}+P_{1v})(I-K_1)^{\mathrm{T}}+ (I-K_1)(a_3I+R_1)(I-K_1)^{\mathrm{T}}+K_1R_2K_1^{\mathrm{T}} \tag{67}$$

$$\mathrm{E}[\tilde{\boldsymbol{v}}_{2|2}\tilde{\boldsymbol{v}}_{2|2}^{\mathrm{T}}] = (I-TK_2)(\bar{\boldsymbol{v}}_1\bar{\boldsymbol{v}}_1^{\mathrm{T}}+P_{1v})(I-TK_2)^{\mathrm{T}}+ a_1I-a_2(K_2+K_2^{\mathrm{T}})+ K_2(R_1+R_2+a_3I)K_2^{\mathrm{T}} \tag{68}$$

$$\mathrm{E}[\tilde{\boldsymbol{p}}_{2|2}\tilde{\boldsymbol{v}}_{2|2}^{\mathrm{T}}] = T(I-K_1)(\bar{\boldsymbol{v}}_1\bar{\boldsymbol{v}}_1^{\mathrm{T}}+P_{1v})(I-TK_2)^{\mathrm{T}}+ a_2(I-K_1)-a_3(I-K_1)K_2^{\mathrm{T}}- (I-K_1)R_1K_2^{\mathrm{T}}+K_1R_2K_2^{\mathrm{T}} = \mathrm{E}[\tilde{\boldsymbol{p}}_{2|2}^{\mathrm{T}}\tilde{\boldsymbol{v}}_{2|2}] \tag{69}$$

4 Relationship between SP and TPD algorithms

The SP track initiation algorithm is Bayesian in nature in the sense that it uses the correct dynamic model involving the process noise and prior information of the maximum speed of a target to specify the prior velocity covariance. Second, the SP track initiation algorithm uses the optimal KF steps to process $\boldsymbol{z}_2$. In contrast, the TPD initiation algorithm is non-Bayesian (maximum likelihood (ML) for Gaussian measurement errors or weighted least square (WLS) for converted Cartesian measurements) in nature. The state estimate and corresponding covariance are purely dependent on the measurements and associated covariances.

While the SP track initiation algorithm leads to a biased estimate for $\hat{\boldsymbol{x}}_{2|2}$ in contrast to the unbiased TPD estimate, this does not necessarily mean it is of lower quality. Typically, bias or lack of it is considered an important feature

of an estimator. However, the mean square error of an estimator is also an important factor in estimator selection. It can be shown[15] that a biased estimator may have lower estimation variability than an unbiased one. In particular, it is often the case that a Bayesian estimator, i.e., one that makes use of all available a priori information and which also minimizes the mean square error is biased[15]. We conjecture that the track initiation problem considered here is one such example. That is, we believe that

$$\Sigma_2^{TPD} - \Sigma_2^{SP} \tag{70}$$

is a positive semi-definite matrix. The proof of the result is the subject of future work.

However, in this section, we show that as the process noise approaches zero and the maximum speed $v_{\max}$ approaches infinity, the SP algorithm approaches the TPD algorithm. That is, when there is no a priori information on the target′s speed and process noise is neglected, the two methods are identical. Thus, the differences between the two methods arise from the use of a priori information and correct dynamic model in the SP approach.

We first show that the SP estimate is unbiased in the limit. Note, when the process noise approaches zero (e. g., $q \to 0$ or $a_m \to 0,\ m = 1, 2, 3$), then using (46) $\sim$ (50), we get

$$\lim_{q\to 0} K_1 = (R_1 + T^2 dI)(R_1 + R_2 + T^2 dI)^{-1} \tag{71}$$

$$\lim_{q\to 0} K_2 = Td(R_1 + R_2 + T^2 dI)^{-1}. \tag{72}$$

Thus, when the process noise approaches zero and the maximum speed approaches infinity ($d \to \infty$), we have

$$\lim_{\substack{q\to 0\\ d\to\infty}} K_1 = \lim_{d\to\infty} (R_1 + T^2 dI)[R_1 + R_2 + T^2 dI]^{-1} = \tag{73}$$

$$\lim_{d\to\infty} \left[\frac{1}{T^2 d}(R_1 + R_2) + I\right]^{-1} = I \tag{74}$$

and

$$\lim_{\substack{q\to 0\\ d\to\infty}} K_2 = \left[\frac{d1}{T}(R_1 + R_2) + TI\right]^{-1} = \frac{1}{T} I \tag{75}$$

Therefore,

$$\lim_{\substack{q\to 0\\ d\to\infty}} \hat{\boldsymbol{x}}_{2|2}^{SP} = \lim_{\substack{q\to 0\\ d\to\infty}} \begin{bmatrix} \boldsymbol{z}_1 + K_1(\boldsymbol{z}_2 - \boldsymbol{z}_1) \\ K_2(\boldsymbol{z}_2 - \boldsymbol{z}_1) \end{bmatrix} = \tag{76}$$

$$\begin{bmatrix} \boldsymbol{z}_2 \\ \dfrac{1}{T}(\boldsymbol{z}_2 - \boldsymbol{z}_1) \end{bmatrix}$$

Comparison of (76) with (39) proves that as the process noise approaches zero and the maximum speed approaches infinity, the SP algorithm state estimate approaches the TPD algorithm state estimate at time t_2 and hence is unbiased.

In the Appendix, we show that when the process noise approaches zero and the maximum speed approaches infinity,

$$\lim_{\substack{q\to 0\\ d\to\infty}} [P_{2|2}^{SP}]_{11} = R_2 \tag{77}$$

$$\lim_{\substack{q\to 0\\ d\to\infty}} [P_{2|2}^{SP}]_{12} = \frac{1}{T} R_2 \tag{78}$$

$$\lim_{\substack{q\to 0\\ d\to\infty}} [P_{2|2}^{SP}]_{22} = \frac{1}{T^2}(R_2 + R_1) \tag{79}$$

Comparison of (76) $\sim$ (78) with (40) proves that as the process noise approaches zero and the maximum speed approaches infinity, the covariance of the SP algorithm approaches that of the TPD algorithm at time t_2.

5 Numerical simulation and results

We consider a target in $3D$ with the NCVM. Each component q of the power spectral densities[2, 14] of the white noise acceleration process noise is chosen to have the same value. We used three values for q, (0.5, 1.0, 2.0) $\mathrm{m^2 s^{-3}}$. A radar sensor measures the range, azimuth, and elevation of the target with measurement error standard deviations of 10 m, 1.0 degree, and 1.0 degree, respectively. The measurement time interval is 2 s. We converted the range, azimuth, and elevation measurements to unbiased Cartesian position measurements and calculated the corresponding covariances using the algorithm in [7]. Then, we compared the two track initiation algorithms using these converted Cartesian measurements and associated covariances using 500 Monte Carlo simulations for each value of q. Figs. 1 and 2 show the root sum (sum over the x, y, and z components) square position and velocity errors at t_2 for $q = 1.0\,\mathrm{m^2 s^{-3}}$. The results are similar for $q = 0.5$ and $2.0\,\mathrm{m^2 s^{-3}}$. Figs. 1 and 2 show that the root sum square (RSS) position and velocity errors from the SP initiation algorithm are consistently lower than those from the TPD initiation algorithm. Specifically, the RSS velocity errors from the SP initiation algorithm are significantly lower than those from the TPD initiation algorithm.

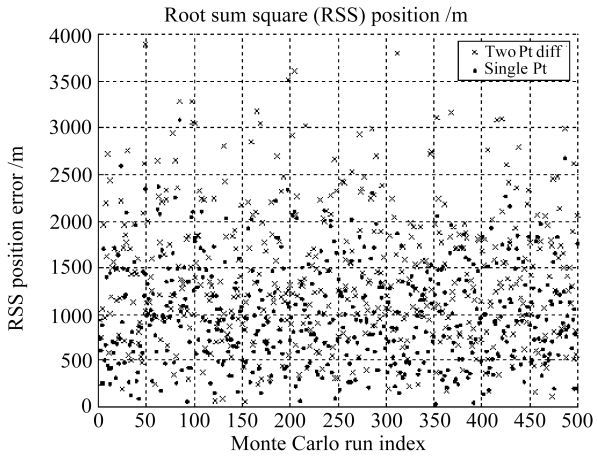

Fig. 1 Root sum square (RSS) position errors from 500 Monte Carlo runs at t_2 from the single-point (SP) and two-point difference (TPD) track initiation algorithms, using q=1.0 $\mathrm{m^2\,s^{-3}}$

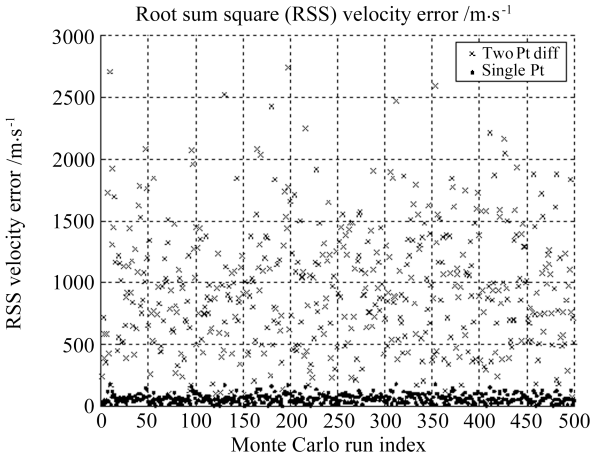

Fig. 2 Root sum square (RSS) velocity errors from 500 Monte Carlo runs at t_2 from the single-point (SP) and two-point difference (TPD) track initiation algorithms, using $q = 1.0\,\mathrm{m^2\,s^{-3}}$

We calculated the MSEM at each observation point ($k = 2, 3, \cdots, 50$) using the SP and TPD initiation algorithms for $q = 0.5, 1.0, 2.0\,\mathrm{m^2\,s^{-3}}$. The MSEM at each observation point is calculated using 500 Monte Carlo runs. The traces of the MSEMs at the observation points $k = 2, 3, \cdots, 50$ are presented in Figs. 3 $\sim$ 5 for three different values of the process noise power spectral density. The ratio of the traces of the MSEMs for the TPD and SP algorithms at t_2 for each value $q = 0.5, 1.0$, or $2.0\,\mathrm{m^2\,s^{-3}}$ is 2.823. We observe that the trace of the MSEM for the SP initiation algorithm is lower than that from the TPD initiation algorithm for the first ten observation points. The traces for these two algorithms become the same afterwards. Thus, if a small number of measurements are available, then it is desirable to use the SP initiation algorithm for higher track initiation accuracy.

The ratio of the traces of the MSEMs from the SP and TPD track initiation algorithms, using $q = 1.0\,\mathrm{m^2\,s^{-3}}$ is presented in Fig. 6. The results are similar for the other two values of q.

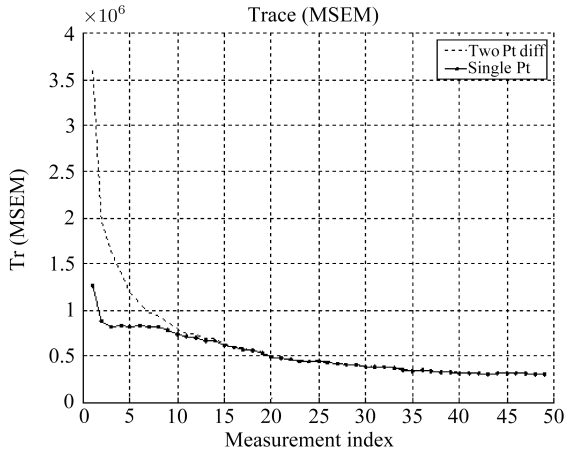

Fig. 3 Comparison of the trace of the MSEM from the SP and TPD track initiation algorithms, with $q = 0.5\,\mathrm{m^2\,s^{-3}}$

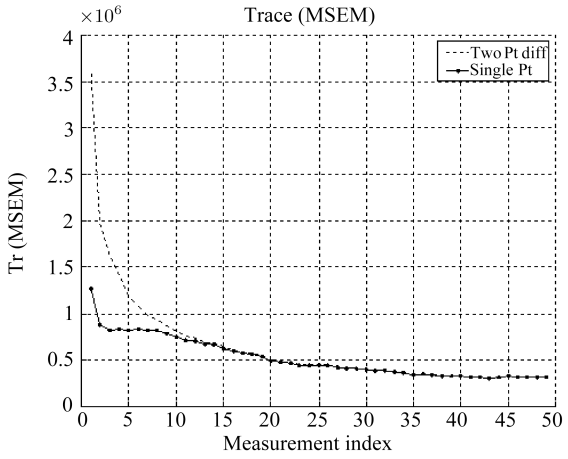

Fig. 4 Comparison of the trace of the MSEM from the SP and TPD track initiation algorithms, with $q = 1.0\,\mathrm{m^2\,s^{-3}}$

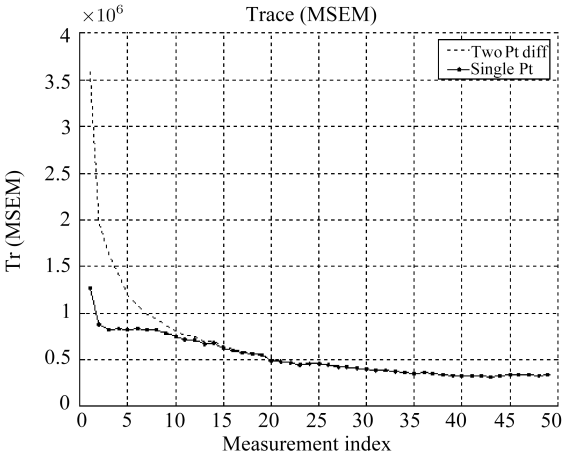

Fig. 5 Comparison of the trace of the MSEM from the SP and TPD track initiation algorithms, with $q = 2.0\,\mathrm{m^2\,s^{-3}}$

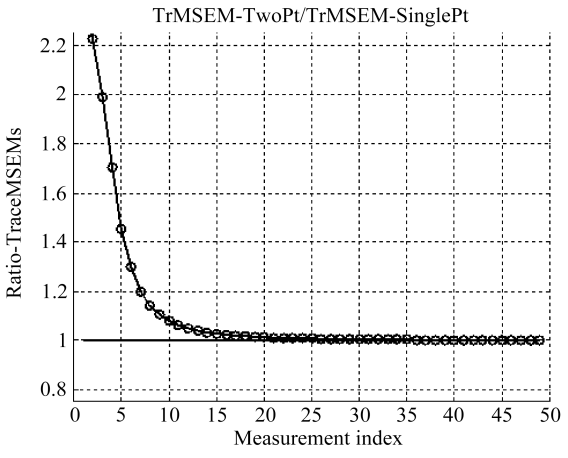

Fig. 6 Ratio of the traces of the MSEMs from the SP and two-point difference TPD track initiation algorithms, using $q = 1.0\,\mathrm{m^2\,s^{-3}}$

6 Conclusion

We have compared the single-point (SP) and two-point difference (TPD) algorithms for initiating a track using the first two position measurements assuming that the dynamic model of the target is the nearly constant velocity model. We have analytically established a connection between these two algorithms. We have shown that, if the process noise approaches zero and the maximum speed of a target used to initialize the velocity variance approaches infinity, then SP algorithm reduces to the TPD algorithm. That is, the differences between the two algorithms are due to the use of additional information in the SP method. The two methods are equivalent when this information is unused or unavailable. As a result, we conjecture that the SP algorithm has a lower mean square error than the more commonly used TPD method. This conjecture is supported by our numerical results from 500 Monte Carlo runs with different levels of process noise. These results show that the SP algorithm with a KF performs consistently better than the TPD algorithm in the mean square error sense.

Acknowledgment

The authors thank Dr. Glenn VanBlaricum of Toyon Research Corporation for help in verifying some of the derivations in the paper using Mathematica.

Appendix

Limiting values of $P_{2|2}^{SP}$

Recall that the state error covariance matrix for the SP algorithm at time t_2 is given by

$$P_{2|2}^{SP} = \begin{bmatrix} A_1 - A_1S^{-1}A_1 & A_2 - A_1S^{-1}A_2 \\ A_2 - A_2S^{-1}A_1 & A_3 - A_2S^{-1}A_2 \end{bmatrix} \tag{A-1}$$

where S is the measurement innovation covariance and

$$A_1 = R_1 + (T^2d + a_3)I \tag{A-2}$$

$$A_2 = (Td + a_2)I \tag{A-3}$$

$$A_3 = (d + a_1)I \tag{A-4}$$

and

$$a_m = \frac{qT^m}{m}, \quad m = 1, 2, 3 \tag{A-5}$$

Therefore,

$$\lim_{q\to 0} A_1 = R_1 + T^2dI \tag{A-6}$$

$$\lim_{q\to 0} A_2 = TdI \tag{A-7}$$

$$\lim_{q\to 0} A_3 = dI \tag{A-8}$$

According to the matrix inversion lemma[1]

$$(A+BCB^{\mathrm{T}})^{-1} = A^{-1} - A^{-1}B(B^{\mathrm{T}}A^{-1}B+C^{-1})^{-1}B^{\mathrm{T}}A^{-1} \tag{A-9}$$

Setting $B = I$, this reduces to

$$(A + C)^{-1} = A^{-1} - A^{-1}(A^{-1} + C^{-1})^{-1}A^{-1} \tag{A-10}$$

Applying (A-10) to S in (47) we get

$$S^{-1} = (A_1 + R_2)^{-1} = A_1^{-1} - A_1^{-1}(A_1^{-1} + R_2^{-1})^{-1}A_1^{-1} \tag{A-11}$$

Using (A-11) in (45), we get

$$\begin{aligned}[P_{2|2}^{SP}]_{11} = {} & A_1 - A_1S^{-1}A_1 = \\ & A_1 - A_1[A_1^{-1} - A_1^{-1}(A_1^{-1} + R_2^{-1})^{-1}A_1^{-1}]A_1 = \\ & A_1 - [I - (A_1^{-1} + R_2^{-1})^{-1}A_1^{-1}]A_1 = \\ & A_1 - [A_1 - (A_1^{-1} + R_2^{-1})^{-1}] = \\ & (A_1^{-1} + R_2^{-1})^{-1}\end{aligned} \tag{A-12}$$

Thus,

$$\begin{aligned}\lim_{\substack{q\to 0\\ d\to\infty}} [P_{2|2}^{SP}]_{11} = {} & \lim_{\substack{q\to 0\\ d\to\infty}} (A_1^{-1} + R_2^{-1})^{-1} = \\ & (R_2^{-1})^{-1} = R_2\end{aligned} \tag{A-13}$$

Similarly, for the cross-covariance component, we get

$$\begin{aligned}[P_{2|2}^{SP}]_{12} = {} & A_2 - A_1S^{-1}A_2 = \\ & A_2 - A_1[A_1^{-1} - A_1^{-1}(A_1^{-1} + R_2^{-1})^{-1}A_1^{-1}]A_2 = \\ & A_2 - [I - (A_1^{-1} + R_2^{-1})^{-1}A_1^{-1}]A_2 = \\ & A_2 - A_2 + (A_1^{-1} + R_2^{-1})^{-1}A_1^{-1}A_2 = \\ & (A_1^{-1} + R_2^{-1})^{-1}A_1^{-1}A_2\end{aligned} \tag{A-14}$$

Thus

$$\begin{aligned}\lim_{\substack{q\to 0\\ d\to\infty}} [P_{2|2}^{SP}]_{12} = {} & \lim_{\substack{q\to 0\\ d\to\infty}} (A_1^{-1} + R_2^{-1})^{-1}A_1^{-1}A_2 = \\ & \lim_{d\to\infty} R_2(T^2dI)^{-1}(TdI) = \frac{1}{T}R_2\end{aligned} \tag{A-15}$$

Finally, using (A-6) in (A-11), we have

$$\lim_{q\to 0} S^{-1} = (R_1 + R_2 + T^2dI)^{-1} \tag{A-16}$$

Combining (A-7), (A-8) and (A-16), we find

$$\begin{aligned}\lim_{\substack{q\to 0\\ d\to\infty}} [P_{2|2}^{SP}]_{22} = {} & \lim_{\substack{q\to 0\\ d\to\infty}} A_3 - A_2S^{-1}A_2 = \\ & \lim_{d\to\infty} dI - T^2d^2(R_1 + R_2 + T^2dI)^{-1} = \\ & \lim_{d\to\infty} dI - T^2d^2(T^{-2}d^{-1})(I + C)^{-1} = \\ & \lim_{d\to\infty} dI - d(I + C)^{-1}\end{aligned} \tag{A-17}$$

where

$$C = \frac{1}{T^2d}(R_1 + R_2) \tag{A-18}$$

Applying the matrix inversion lemma in we get

$$(I + C)^{-1} = I - (I + C^{-1})^{-1} \tag{A-19}$$

Substitution of (A-18) and (A-19) into (A-17) gives

$$\begin{aligned}\lim_{\substack{q\to 0\\ d\to\infty}} [P_{2|2}^{SP}]_{22} = {} & \lim_{d\to\infty} dI - dI + d(I + C^{-1})^{-1} = \\ & \lim_{d\to\infty} (\frac{1}{d}I + \frac{1}{d}C^{-1})^{-1} = \\ & [T^2(R_1 + R_2)^{-1}]^{-1} = \\ & \frac{1}{T^2}(R_1 + R_2)\end{aligned} \tag{A-20}$$

References

1 Anderson B D O, Moore J B. *Optimal Filtering*. New Jersey: Prentice-Hall, 1979

2 Bar-Shalom Y, Li X R, Kirubarajan T. *Estimation with Applications to Tracking and Navigation*. New York: John Wiley and Sons, 2001

3 Fitzgerald R J. Divergence of the Kalman filter. *IEEE Transactions on Automatic Control*, 1971, **16**(6): 736−747

4 Heffes H. The effect of erroneous models on the Kalman filter response. *IEEE Transactions on Automatic Control*, 1966, **11**(3): 541−543

5 Soong T T. On *a priori* statistics in minimum variance estimation problems. *Journal of Basic Engineering, Transactions of the American Society of Mechanical Engineers (ASME)*, 1965, **87**D: 109−112

6 Li X R, He C. Optimal initialization of linear recursive filters. In: Proceedings of the 37th IEEE Conference on Decision and Control. Tampa, USA: IEEE, 1998. 2335−2340

7 Mo L B, Song X Q, Zhou Y Y, Sun Z K, Bar-Shalom Y. Unbiased converted measurements for tracking. *IEEE Transactions on Aerospace and Electronic Systems*, 1998, **34**(3): 1023−1027

8 Mallick M. Maximum likelihood geolocation using a ground moving target indicator (GMTI) report. In: Proceedings of 2002 IEEE Aerospace Conference. Big Sky MT, USA: IEEE, 2002. 1561−1570

9 Mallick M. Geolocation using video sensor measurements. In: Proceedings of the 10th International Conference on Information Fusion. Quebec, Canada: IEEE, 2007.

10 Tian X, Bar-Shalom Y. Coordinate conversion and tracking for very long range radars. In: Proceedings of Radar Resolution, Nonlinear Estimation and Other Gratuitous Remarks on the Back of an Envelope: A Tribute to Fred Daum. Monterey, USA: 2007

11 Mallick M, Kirubarajan T, Arulampalam S. Comparison of nonlinear filtering algorithms in ground target indicator (GMTI) tracking. In: Proceedings of the 4th International Conference on Information Fusion. Montreal, Canada: 2001

12 Mallick M, Arulampalam S. Comparison of nonlinear filtering algorithms in ground moving target indicator (GMTI) target tracking. In: Proceedings of SPIE Conference on Signal and Data Processing of Small Targets. Orlando, USA: SPIE, 2004. 630−647

13 Jazwinski A H. *Stochastic Processes and Filtering Theory*. New York: Academic Press, 1970

14 Gelb A. *Applied Optimal Estimation*. Cambridge: MIT Press, 1974

15 DeGroot M H. *Probability and Statistics (Second Edition)*. California: Addison-Wesley, 1987

MALLICK Mahendra Chief scientist at Science Applications International Corp. (SAIC) in San Diego, USA. He received his Ph. D. degree in solid state theory from the State University of New York at Albany in 1981. He has over twenty-five years of professional experience including employment at Toyon Research Corp. (2005 − 2007), Lockheed Martin ORINCON (2003−2005), ALPHATECH Inc. (1996 − 2002), TASC (1985−96) and CSC (1981−85). His research interests cover estimation, stochastic modeling, multi-sensor multi-target tracking, joint tracking and classification, nonlinear filtering, particle filtering, out-of-sequence measurement and track algorithms, electromagnetic scattering, orthogonal distance regression, motion estimation, data registration, data fusion, satellite orbit and altitude estimation, numerical computation, and object oriented analysis and design. He is a senior member of the IEEE and a member of the International Society for Information Fusion (ISIF). Corresponding author of this paper.
E-mail: mahendra.mallick@gmail.com

LA SCALA Barbara Received her Ph. D. degree in systems engineering from the Australian National University in 1994. She is currently a member of the Melbourne Systems Laboratory in the Electrical and Electronic Engineering Department at the University of Melbourne, Australia. Her research interests cover estimation, optimal sensor scheduling, and management of distributed systems. She has worked on a number of DSTO and DARPA funded projects in these areas. Before joining MSL she worked for RLM Pty Ltd designing target tracking and sensor registration algorithms for Australia′s Jindalee Over-the-horizon Radar Network (JORN). In addition to her position as assistant editor-in-chief of the *Journal of Advances in Information Fusion* (JAIF), she is also an associate editor of the *IEEE Transactions on Aerospace and Electronic Systems* for papers on target tracking and multi-sensor systems.
E-mail: b.lascala@ee.unimelb.edu.au